Indonesian Journal of Material Research
e-ISSN: 2987-1654
Vol. 4, No. 3, November 2026

Indonesian Journal of MATERIAL RESEARCH

Research Paper

Adsorption of Methyl Orange from Aqueous Solution using Ni/Al LDH Modified with *Camellia sinensis* Leaf Extracts

Amri Amri[1*], Heroldinho Arieveali[1]

[1] *Research Center of Inorganic Materials and Coordination Complexes, Universitas Sriwijaya, Palembang, 30139, Indonesia*
[*]**Corresponding author**: amrikd07@gmail.com

Abstract
Water pollution caused by dye pollutants such as methyl orange (MO) can have a negative impact on humans, living organisms, and ecosystems. Adsorption is one of the promising methods in overcoming the presence of MO pollutants. This research focuses on the synthesis of layered double hydroxide (LDH) Ni/Al composites prepared by coprecipitation method with the addition of green tea/*Camellia sinensis* (CS) leaf extract as supporting material. The synthesized materials obtained were then characterized using X-ray diffraction (XRD) patterns and Fourier transform infrared spectra (FTIR). The Ni/Al and Ni/Al-CS materials were then evaluated as adsorbents to adsorb MO from aquatic solutions. The maximum capacity of MO adsorption obtained was 18.519 mg.g^{-1} on Ni/Al LDH and 49.261 mg.g^{-1} on Ni/Al-CS, respectively. The Langmuir isotherm model showed the best fit to the adsorption data on both materials, while the kinetics of the adsorption process followed a pseudo second-order (PSO) model. Thermodynamic analysis (ΔG°, ΔS°, and ΔH°) showed that the MO adsorption process on both materials was spontaneous and endothermic. The regeneration process carried out four consecutive regeneration cycles showed that Ni/Al-CS material has excellent adsorbent recycling ability, which only decreased by 10.26%. In contrast to Ni/Al LDH which experienced a significant decrease of up to 31.70% in the 4th cycle. These findings suggest that Ni/Al-CS material is a promising adsorbent for MO removal applications from aquatic solutions.

Keywords
Ni/Al LDH, *Camellia sinensis*, Composite, Adsorption, Methyl Orange

Received: 27 February 2026, Accepted: 9 April 2026
https://doi.org/10.26554/ijmr.20264393

1. INTRODUCTION

Water pollution has become a global problem that has increased significantly in recent decades. The growth of the industrial sector, increasing population, and rapid urbanization are the main factors contributing to the escalation of water pollution in many parts of the world (Wibiyan et al., 2024). Various new pollutants have been identified in the aquatic environment, including persistent organic pollutants, plastics, solvents, dyes, paints, and other compounds (Dehmani et al., 2025). Dye is one of the commonly found contaminants that contribute significantly to water pollution and is widely used in various industries, such as textiles, paints, plastics, pulp and paper, printing, cosmetics, pharmaceuticals, and food processing (Abd Al-khuder and Karam, 2025; Hosseinpour and Rahbar-Kelishami, 2025).

Methyl orange (MO) is one example of a hazardous anionic azo dye that can have a significant negative impact on the ecosystem. It has mutagenic and carcinogenic properties that can harm all living organisms. In addition, long-term exposure to MO in humans can cause various health problems, such as allergic skin diseases, respiratory problems, asthma, changes in immunoglobulin levels, increased risk of cancer, tumors in the bladder, and liver (Ahmad et al., 2024a; El Foulani et al., 2025; Pan et al., 2025; Yang et al., 2024). Therefore, it is necessary to remove the presence of MO dyes in wastewater to prevent negative impacts on ecosystems and human health.

Various strategies have been applied to remove heavy metals and dyes from wastewater, including chemical precipitation, ion exchange, photodegradation, membrane filtration, coagulation-flocculation, and adsorption (Alsaab et al., 2025; Mishra et al., 2024; Popat et al., 2024; Waheed et al., 2024). Among these methods, adsorption has attracted much attention due to its high efficiency, relatively low cost, as well as its application flexibility, thus making it one of the promising solutions to address pollution caused by MO dyes (Amri et al., 2024; Lesbani et al., 2024; Xie et al., 2024).

Layered Double Hydroxides (LDH) are anionic clay materials that have a two-dimensional layered structure composed of interactions between the positive charges of divalent (M^{2+}) and trivalent (M^{3+}) metal ions, hydroxyl groups, and interlamellar anions (Ahmad et al., 2024b; Amri et al., 2023). LDH has several

advantages including easy synthesis process, good specific surface area, and large ion exchange capacity, which is favorable especially in terms of adsorption of anionic pollutants (Boucif et al., 2025; Jin et al., 2025). Despite its many advantages, pure LDH still faces a few limitations, such as the tendency to aggregate, low mechanical stability, and difficulty in regeneration. This has encouraged researchers to explore the formation of composite materials as a solution to overcome these limitations (Mubarak et al., 2025). Research conducted by Wijaya et al. (2025) modified NiCr LDH by composite with *Spirogyra sp.* algae (NiCr-SA) for reactive red adsorption resulting in an increase in the maximum adsorption capacity from 11.976 mg/g (NiCr LDH) to 47.170 mg/g (NiCr-SA). Hammood and Mohammed (2024) modified CaMgAl LDH by composite with red mud for tetracycline adsorption resulting in a stable material that can be used six regeneration cycles sequentially and only a 27% decrease in removal efficiency.

Green tea (*Camellia sinensis* (CS)) leaves have been recognized as a promising biosorbent due to their abundant availability, low cost, and the presence of active functional groups that support the adsorption process. Phenolic compounds such as flavanols (catechins, gallic acid, flavonoids, and others) contained in green tea leaf extract are expected to contribute to the enhancement of adsorption ability (Etim et al., 2024; Roy et al., 2022).

In this study, Ni/Al LDH composites modified with CS leaf extract were synthesized using the coprecipitation method. The synthesized materials were then thoroughly characterized using X-ray diffraction (XRD) and Fourier transform infrared spectroscopy (FTIR). Furthermore, the adsorption process of MO dye was tested by varied solution pH, contact time to study adsorption kinetics, as well as temperature and concentration to analyze isotherms and thermodynamics. In addition, regeneration tests were conducted to assess the stability and reusability of the composite as an adsorbent.

2. EXPERIMENTAL

2.1 Chemicals and Instrumentation

The materials used in this study include green tea leaves (*Camellia sinensis*) which were purchased commercially and came from the Dempo Mountains, South Sumatra (Indonesia). The chemical reagents used included nickel nitrate hexahydrate ($Ni(NO_3)_2.6H_2O$), aluminum nitrate nonahydrate ($Al(NO_3)_3.9H_2O$), sodium hydroxide (NaOH), HCl (Hydrochlorid Acid), and sodium chloride (NaCl) obtained from SigmaAldrich. Ethanol (C_2H_5OH) technical 96% was purchased from BIMO ANALYSIS, Indonesia. Distilled water was obtained from BrataChem, Indonesia and methyl orange dye samples were also used in this study. Characterization instruments used include Rigaku MiniFlex 600 X-Ray Diffractometer (XRD), Shimadzu Prestige-21 Fourier Transform Infrared spectrophotometer (FT-IR). Analytical instruments were used with Biobase BK-UV 1800 PC series UV-Vis spectrophotometer.

2.2 Synthesis of Ni/Al LDH (Lesbani et al., 2024)

Ni/Al LDH was synthesized using the coprecipitation method. The precursor solution was prepared by mixing nickel nitrate hexahydrate ($Ni(NO_3)_2.6H_2O$) 0.75 M and aluminum nitrate nonahydrate ($Al(NO_3)_3.9H_2O$) 0.25 M in a Ni^{2+}/Al^{3+} molar ratio of 3:1. The mixture was stirred continuously while adding 2 M NaOH solution dropwise until the pH of the system reached 10. The mixture was then stirred for 12 hours at 80°C. The precipitate formed was separated, washed with distilled water until neutral, and then dried in an oven to obtain Ni/Al LDH powder.

2.3 Green Tea (*Camellia sinensis*) Leaf Extraction

The CS leaf extract was carried out with slight modifications that have been carried out by Han et al. (2024). Green tea (*Camellia sinensis*) leaves were dried and pulverized before extraction. The extraction process was carried out through maceration method using 96% ethanol solvent. The dried leaf samples were immersed in the solvent and remaining for 1 hour. After the maceration process was complete, the solution was filtered and the solvent was separated using a rotary evaporator at 48°C to obtain a concentrated extract of CS, which was then stored at low temperature until further use.

2.4 Preparation of Ni/Al-CS Composites

The Ni/Al-CS composite was synthesized via a coprecipitation method with modification using natural materials. The preparation of Ni^{2+} and Al3+ precursors was carried out following the same procedure as in the previously described LDH synthesis. The metal precursor solution was prepared and stirred under appropriate conditions, after which 0.5 g of CS extract was introduced into the system. A 0.5 M NaOH solution was then added dropwise until the desired pH was achieved, and the mixture was continuously stirred for 24 h to ensure homogeneity and complete precipitation. The resulting suspension was aged to facilitate precipitate formation, followed by filtration and washing with distilled water until neutral pH was obtained. The solid product was then dried in an oven to yield the Ni/Al-CS composite powder.

2.5 Determination of pH Point Zero Charge (pHpzc) on Each Adsorbent

The surface charge characteristics of the material in a neutral state can be determined through the pHpzc value. This determination was made by preparing 20 mL of 0.1 M NaCl solution which was adjusted to pH in the range of 2 to 10 using HCl and NaOH solutions. A total of 0.02 g of Ni/Al LDH and Ni/Al-CS materials were added separately to the solution, then stirred for 24 hours. Afterwards, the final pH of the solution was measured to calculate ΔpH (the difference between the initial pH and the final pH). The ΔpH data was then plotted against the initial pH to determine the pHpzc value.

2.6 Adsorption of MO

Adsorption studies were conducted to evaluate the effect of various parameters on the MO dye removal process, including variations in pH, contact time (for kinetics studies), temperature

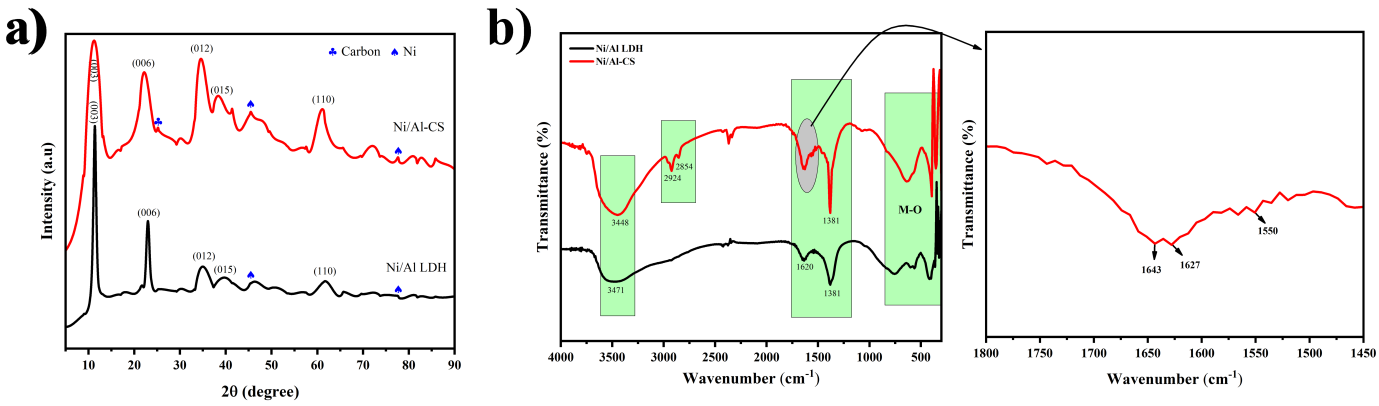

Figure 1. Material Characterization Using XRD (a) and FT-IR Spectra (b)

and concentration (for isotherm and thermodynamic analysis), as well as the regeneration process in adsorbent reuse. In each experiment, 20 mL of MO solution was mixed with 0.02 grams of each adsorbent. The effect of pH was studied by adjusting the pH of the solution from pH 5 to pH 10. The effect of time in the kinetics study was carried out by varying the contact time at intervals of 0, 15, 30, 45, 60, 75, 90, 105, 120, 135, 150, 165 and 180 minutes. The effect of temperature and concentration was studied using concentration variations of 35, 40, 45, and 50 mg/L at a temperature range of 30°C to 50°C. Regeneration in adsorbent reuse was performed for four adsorption-desorption cycles.

3. RESULTS AND DISCUSSION

3.1 Characterization of the Adsorbent Materials

The XRD spectra of Ni/Al LDH and Ni/Al-CS can be seen in Figure 1(a). The XRD spectrum of the Ni/Al LDH material shows several distinct peaks referring to JCPDS data no. #15-0087 indicating the presence of a multilayer hydrotalcite structure with angles 2θ = 11.34°, 22.93°, 34.86°, 39.55°, 45.50°, and 61.67° corresponding to planes (003), (006), (012), (015), (018), and (110) (Duddi et al., 2025; Martins and Perez-Lopez, 2025). In Ni/Al-CS, there is an additional peak that appears at an angle of 2θ = 25.30° with an amorphous structure that shows the presence of CS extract in the composition of Ni/Al-CS material (Hezari et al., 2022). In addition, the peaks appearing on Ni/Al LDH and Ni/Al-CS at angles 2θ = 45°, 48° and 77.61° with (111) and (220) planes indicate the presence of the crystalline phase of Ni metal (JCPDS no. #04-0850) (Ma et al., 2022).

The FTIR spectra of Ni/Al LDH and modified with the addition of CS leaf extract can be seen in Figure 1(b). In Ni/Al LDH, there is a broad peak at wave number 3471 cm^{-1} which is associated with O-H stretching vibrations of hydroxyl groups in the LDH structure. The peak at 1381 cm^{-1} indicates the presence of nitrate anion (NO_3^-) in the interlayer of LDH (Borah et al., 2025). The absorption band obtained at 1620 $^{-1}$ indicates the presence of −OH bending virbation obtained from H_2O molecules between layers (Hariprasath et al., 2024). All peaks generated from wavenumbers <1000 cm^{-1} indicate the presence of metal vibrations with oxygen lattice (Ni−O, Al−O) (Hariprasath et al., 2024; Li et al., 2022).

Ni/Al-CS material is a modified Ni/Al LDH material with the addition of CS leaf extract from Ni/Al-CS can be seen the typical absorption peak of tea leaf extract. The broad band at 3448 cm^{-1} shows the O−H stretching vibrations associated with the LDH structure and the O−H groups of polyols, phenols, and alcohols in the CS leaf extract. The absorption bands at 2924 and 2854 cm^{-1} indicate symmetric and asymmetric stretching of the C−H bond in the methyl group. Absorption bands at 1643, 1627, and 1550 cm^{-1} indicating C=O, C=N, and C=C stretching vibrations in cyclic hydrocarbons. In addition, the three absorption peaks are characteristic of caffeine, which is the most abundant component in CS leaf extract (Milovanovic et al., 2024). The results showed that the synthesis of Ni/Al LDH and the modification of Ni/Al-CS materials were successfully carried out.

3.2 Adsorption Study

pHpzc is used to determine the pH point where the surface charge of the material is zero/neutral (Ahmad et al., 2025; Hashem et al., 2025). The pHpzc value of each material is 7.9 for Ni/Al LDH and 7.4 for Ni/Al-CS (Figure 2(a)). Both materials are expected to have a positively charged surface when pH<pHpzc, a negatively charged surface when pH>pHpzc, and a zero charged surface when both materials when pH=pHpzc (Tcheka et al., 2024).

Considering that MO is an anionic dye, the adsorption process that occurs at pH <PHpzc is preferred due to the electrostatic attraction that occurs between the positively charged material surface and the dye molecules. Based on the results obtained, Ni/Al LDH material has high adsorption ability at pH 5 and Ni/Al-CS at pH 6 (Figure 2(b)). This indicates the process of electrostatic attraction, while at pH>pHpzc there is a decrease in adsorption ability due to electrostatic repulsion.

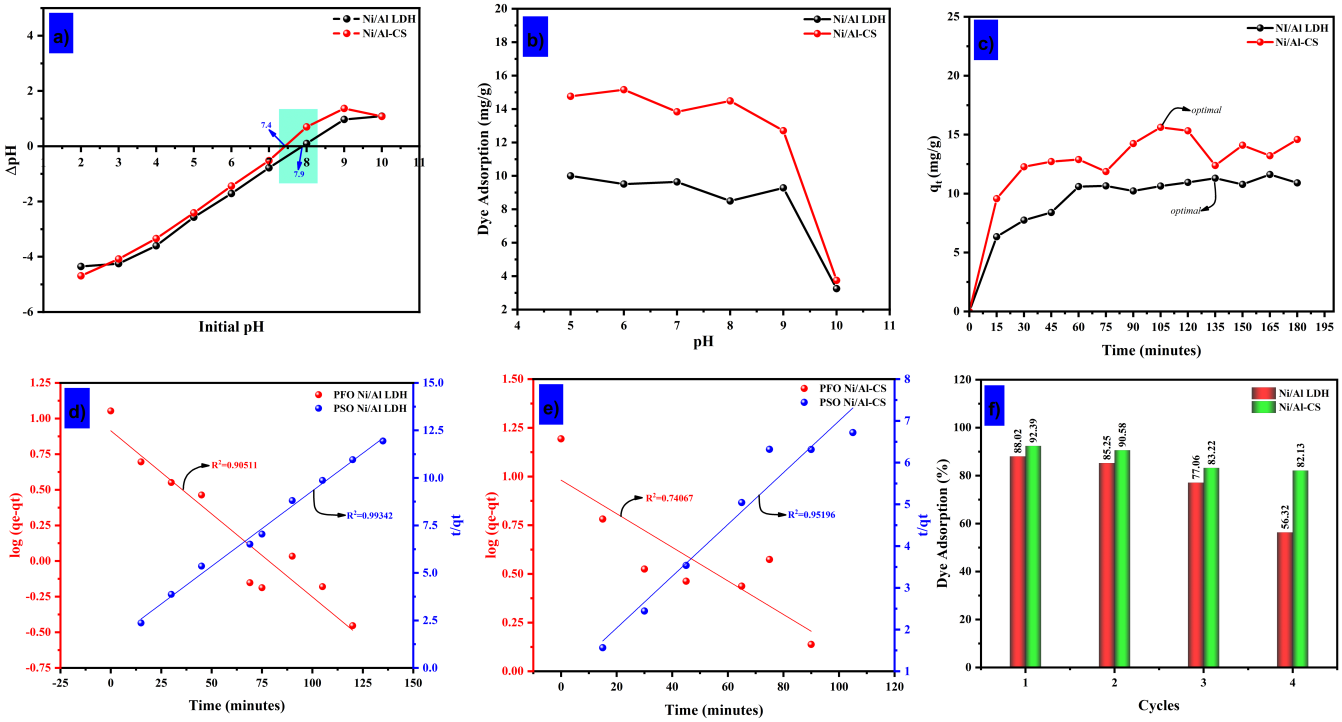

Figure 2. Determination of Adsorbent pHpzc (a), Effect of pH (b) and Contact Time (c) on MO Adsorption, Modeling of Adsorption Kinetics Using PFO and PSO Models for Ni/Al LDH (d) and Ni/Al-CS (e), and Study of Adsorbent Regeneration in the Adsorption Process (f)

The effect of time on MO adsorption on Ni/Al LDH and Ni/Al-CS materials can be seen in Figure 2(c). In the figure, it can be seen that a rapid adsorption phase is observed during the first 60 minutes, which is mainly due to the large number of active sites on the Ni/Al surface as well as the high initial concentration of MO in the solution (Leng et al., 2025). Subsequently, the adsorption rate tends to rise and fall gradually between 60 to 135 minutes, until finally reaching the adsorption equilibrium condition after 135 minutes. Similarly, Ni/Al-CS underwent a rapid adsorption phase up to 105 minutes and experienced equilibrium and the adsorption rate fluctuated after 105 minutes. This is due to the reduction of the active sites of the material to adsorb MO, which in turn has an impact on inhibiting the adsorption rate (Duan et al., 2025; Leng et al., 2025).

The kinetics of MO adsorption on Ni/Al LDH and Ni/Al-CS were analyzed using various kinetic models, including pseudo first order (PFO) and pseudo second order (PSO) as shown in Figure 2(d-e). The kinetic parameters obtained from both models are summarized in Table 1. Both materials show that the pseudo second order model has the best fit with a higher correlation coefficient (R^2) than the pseudo first order model. In addition, the qe calculated values in PSO in both materials (Ni/Al LDH = 12.610, Ni/Al-CS = 16.129) are very similar to the qe exp values (Ni/Al LDH = 11.303, Ni/Al-CS = 15.624). These results indicate that the pseudo second order kinetic model is more accurate in describing the adsorption behavior of MO dye on Ni/Al LDH and Ni/Al-CS materials, and indicate that the chemisorption process plays a dominant role in the adsorption mechanism (Qiu et al., 2025).

Table 1. Kinetics Parameters of MO Adsorption on Ni/Al LDH and Ni/Al-CS

	Ni/Al LDH	Ni/Al-CS
Pseudo first order		
k_1 (min^{-1})	0.027	0.020
q_e (calc) (mg/g)	8.204	9.590
R^2	0.905	0.741
Pseudo second order		
k_2 (min.g/mg)	0.0045	0.0048
q_e (calc) (mg/g)	12.610	16.129
R^2	0.993	0.952
q_e (exp)	11.303	15.624

In this study, the adsorption isotherm behavior of MO dye on Ni/Al LDH and Ni/Al-CS materials was evaluated using two adsorption isotherm models, namely Langmuir isotherm and Freundlich isotherm. These models are important to understand how the adsorbate interacts with the adsorbent and provide

Table 2. Isotherm Parameters of MO Adsorption using Ni/Al LDH and Ni/Al-CS

Materials	T (K)	Parameters			
		Isotherm Langmuir		Isotherm Freundlich	
Ni/Al LDH	303	q_{max} (mg.g^{-1})	18.519	n	1.743
				$1/n$	0.574
		KL (L.mg^{-1})	0.377	KF [(mg.g^{-1})(L.mg^{-1})$^{1/n}$]	98.855
		R^2	0.983	R^2	0.7491
Ni/Al-CS	303	q_{max} (mg.g^{-1})	49.261	n	6.061
				$1/n$	0.165
		KL (L.mg^{-1})	0.967	KF [(mg.g^{-1})(L.mg^{-1})$^{1/n}$]	30.889
		R^2	0.9558	R^2	0.434

Table 3. Maximum Adsorption Capacity of MO Dye Adsorption with Different Adsorbents

Adsorbent	q_{max} (mg/g)	Reference
Iron peanut shell-based biochar	6	(Dong et al., 2024)
Iron rice husk-based biochar	17.2	(Dong et al., 2024)
Corn Straw	10	(Fu et al., 2023)
Modified clay with CTAB surfactant	15.58	(Abbou et al., 2023)
Orange and lemon peels-derived activated carbon	38	(Ramutshatsha-Makhwedzha et al., 2022)
Chitosan bead-like materials	14.29	(Alyasi et al., 2023)
Modified fly ash-based geopolymer	19.231	(Purbasari et al., 2023)
Ni/Al LDH	18.519	This work
Ni/Al-CS	49.261	This work

valuable parameters to describe the adsorption process (Alsaab et al., 2025). A complete summary of MO adsorption isotherm parameters is presented in Table 2. The results show that the experimental data best fit the Langmuir isotherm model, which provided higher R^2 values compared to the Freundlich isotherm model (Zhang et al., 2025). The Langmuir isotherm model describes the adsorption process occurring in a monolayer on the adsorbent surface, where adsorption occurs only on certain sites without any lateral interactions or steric constraint between molecules. This indicates that all active sites have equal energy and are independent (Sajai et al., 2025).

In addition, the Langmuir isotherm model resulted in a maximum adsorption capacity (q_{max}) of 49.261 mg.g^{-1} on Ni/Al-CS, which is 2.66 times higher than that of Ni/Al LDH (18.519 mg.g^{-1}). Comparison of the maximum adsorption capacity value of this study with other studies can be seen in Table 3. Notably, the KL value (Ni/Al-CS = 0.967) obtained from the Langmuir model is in the range of 0 to 1, while the 1/n value (Ni/Al-CS = 0.165) in the Freundlich model is in the range of 0.1-0.5, which indicates that the Ni/Al-CS material has good adsorption affinity and a heterogeneous surface (Zhou et al., 2025). In addition, a higher KL value indicates a stronger bonding ability between the adsorbent and adsorbate, while a higher n value indicates a stronger interaction between the two components (Alsaab et al., 2025).

Thermodynamic parameters such as enthalpy change (ΔH°), entropy (ΔS°), and Gibbs free energy (ΔG°) were used to understand the nature and spontaneity of the methyl orange (MO) adsorption process on Ni/Al LDH and Ni/Al-CS materials (Table 4). The values of ΔH° and ΔS° were calculated from the slope and intercept of the Van't Hoff linear plot, while ΔG° was determined using the Equation (Alsaab et al., 2025):

$$\Delta G^\circ = \Delta H^\circ - T\Delta S^\circ$$

As shown in Table 4, the ΔH° values for both materials are positive, namely 17.942 kJ/mol for Ni/Al LDH and 13.006 kJ/mol for Ni/Al-CS, indicating that the adsorption process is endothermic. The increasingly negative increase in ΔG° values as temperature increases (from 303 K to 323 K) indicates that the adsorption process becomes more spontaneous at higher temperatures. This confirms that an increase in temperature is favorable for the MO adsorption process in both materials.

The positive ΔS° values (0.066 and 0.054 kJ/mol.K for Ni/Al LDH and Ni/Al-CS, respectively) indicated an increase in disorder at the solid-liquid interface during the adsorption process. The negative ΔG° values at all temperatures tested confirmed that the adsorption of MO on Ni/Al LDH and Ni/Al-CS was spontaneous. In addition, ΔH° values in the range of 2-40 kJ/mol indicate that the dominant adsorption mechanism is likely to be physical (physisorption) such as van der Waals forces or electrostatic interactions, although the involvement of mild chemical interactions cannot be completely discounted.

An effective adsorbent must not only have a high adsorption capacity, but also the ability to be regenerated. Regeneration is a crucial factor in the sustainable and economical use of adsorbents (El Foulani et al., 2025). To evaluate the regeneration potential,

Table 4. Thermodynamic Parameter Values for MO Adsorption on Ni/Al LDH and Ni/Al-CS

Materials	ΔH° (kJ/mol)	ΔS° (kJ/mol.K)	ΔG° (kJ/mol)		
			303	313	323
Ni/Al LDH	17.942	0.066	-2.038	-2.698	-3.357
Ni/Al-CS	13.006	0.054	-3.381	-3.922	-4.463

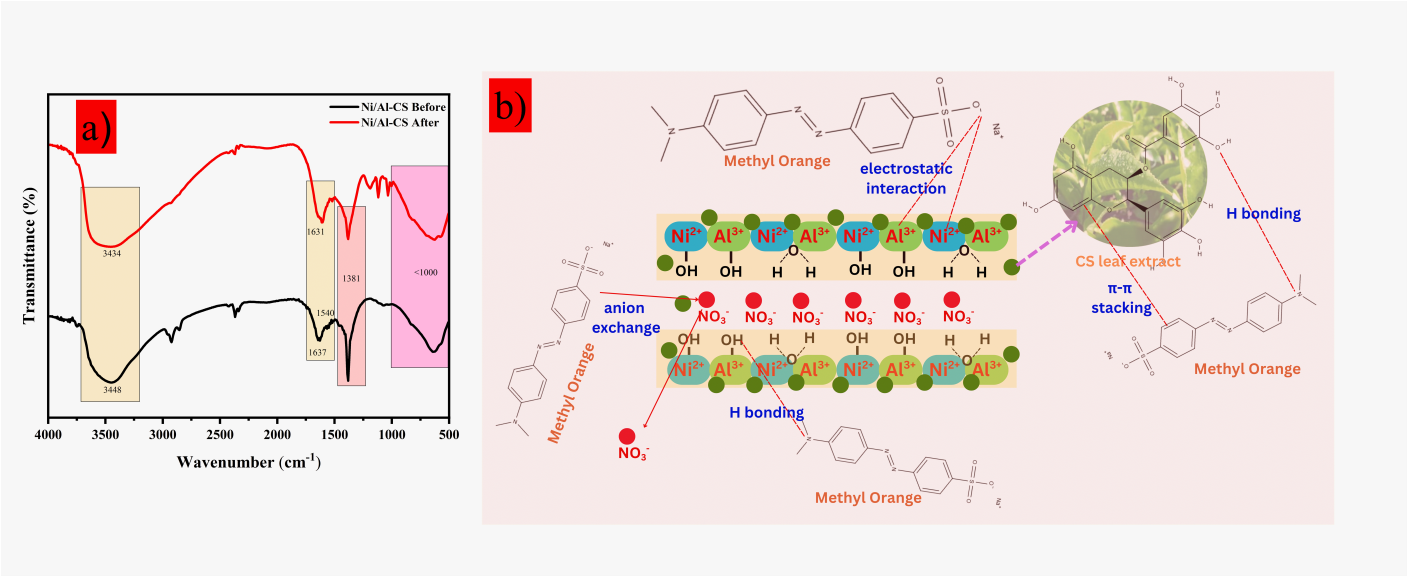

Figure 3. FT-IR Spectra Before and After Adsorption (a) and the Adsorption Mechanism of MO Dye (b)

we conducted four cycles of consecutive adsorption on MO under optimum conditions. As shown in Figure 2(f), the efficiency of adsorption on Ni/Al-CS remained relatively stable over the four cycles, with a decrease in MO adsorption capacity of only 10.26% in the last cycle. Meanwhile, Ni/Al LDH experienced a significant decrease in MO adsorption capacity of 31.70% in the last cycle. These findings indicate that Ni/Al-CS has excellent adsorbent recyclability after repeated treatment.

3.3 Mechanism of Adsorption

Based on the results of the study of the effect of pH and the value of the point of zero charge (pHpzc), it was concluded that the maximum adsorption of MO dye occurred under the condition of solution pH < pHpzc. Under these conditions, the surface of the Ni/Al-LDH material modified with CS leaf extract (Ni/Al-CS) is positively charged, so it is able to have electrostatic interaction with the negatively charged sulfonate group ($-SO_3^-$) of MO dye. It can also be seen that changes in the <1000 cm^{-1} band indicate the involvement of M−O groups (Ni−O and Al−O) in surface interactions (Figure 3(a)). Based on Figure 3(a), it can be seen the FT-IR spectra of Ni/Al-CS before and after MO adsorption. After MO adsorption, there is a shift in the main bands indicating the interaction between the active groups of the adsorbent and the dye molecules. The −OH band shifted from 3448 to 3434 cm^{-1} with a slight decrease in intensity, indicating the formation of hydrogen bonds between the hydroxyl groups of the polyphenolic compounds and the azo or sulfonate groups of MO. The band at 1637 cm^{-1} shifted to 1631 cm^{-1}, indicating an interaction between the aromatic or carbonyl groups of the compounds in the tea extract with the aromatic structure of MO. The decrease in intensity at 1540 cm^{-1} band also indicates the participation of C=O groups or aromatic rings in the π-π stacking interaction. In addition, the absorption band at 1381 cm^{-1} derived from the symmetrical stretching vibration of nitrate anion (NO_3^-) showed a decrease in intensity after the adsorption process. This indicates the partial exchange of NO_3^- anion in the LDH interlayer space by the negatively charged MO molecules. This phenomenon strengthens the anion exchange-based adsorption mechanism, where MO anions are associated with positively charged surfaces or enter into the interlayer space replacing NO_3^- anions. In general, the mechanism of MO adsorption on Ni/Al-CS can be seen in Figure 3(b).

4. CONCLUSIONS

This study successfully prepared Ni/Al LDH material modified with *Camellia sinensis* (S) leaf extract through coprecipitation method as adsorbent for MO removal from aquatic solution as confirmed by XRD and FTIR data. The Ni/Al-CS material has a maximum adsorption capacity of 49.261% mg.g-1 which is 2.66 times greater than Ni/Al LDH. The isotherm and kinetics models showed that both materials followed the Langmuir and PSO isotherm models. Thermodynamic parameters confirmed that

the process was spontaneous and endothermic. Good material stability was also demonstrated for Ni/Al-CS through regeneration cycles, with only 10.26% efficiency loss after four reuses. These findings confirm the potential application of Ni/Al-CS as an efficient, sustainable and reliable adsorbent for the mitigation of MO contamination in aquatic systems.

5. ACKNOWLEDGEMENT

The authors would like to express their appreciation for the support and instrumental analysis facilities provided by the Research Center of Inorganic Materials and Coordination Complexes, Universitas Sriwijaya, which have contributed in supporting the completion of this research.

REFERENCES

Abbou, B., I. Lebkiri, H. Ouaddari, A. El Amri, F. E. Achibat, L. Kadiri, A. Ouass, A. Lebkiri, and E. H. Rifi (2023). Improved Removal of Methyl Orange Dye by Adsorption Using Modified Clay: Combined Experimental Study Using Surface Response Methodology. *Inorganic Chemistry Communications*, **155**; 111127

Abd Al-khuder, Z. H. and F. F. Karam (2025). Synthesis and Characterization of a Quaternary Composite Based on RGO/MWCNTs/Choline Chloride + Malonic Acid for Methyl Orange Dye Adsorption. *Results in Chemistry*, **15**; 102133

Ahmad, N., S. P. J. Negara, et al. (2024a). Insight of Anionic Dyes Adsorption from Their Aqueous Solutions onto MgAl LDH/Lignin: Characterization and Isotherm Studies. *Indonesian Journal of Material Research*, **2**(2); 40–46

Ahmad, N., A. Wijaya, A. Lesbani, et al. (2024b). Magnetite Humic Acid-Decorated MgAl Layered Double Hydroxide and Its Application in Procion Red Adsorption. *Colloids and Surfaces A: Physicochemical and Engineering Aspects*, **684**; 133042

Ahmad, N., A. Wijaya, et al. (2025). Comparative Assessment of Procion Red Removal Using Magnetite-Based Composites with Humic Acid, Activated Charcoal, and Lignin. *Indonesian Journal of Material Research*, **3**(3); 85–92

Alsaab, H. O., S. Shirazian, N. Pirestani, and R. Soltani (2025). Sustainable Synthesis and Dual Adsorption of Methyl Orange and Cadmium Ions Using Biogenic Silica-Based Fibrous Silica Functionalized with Crown Ether Ionic Liquid. *Journal of Colloid and Interface Science*, **679**; 555–568

Alyasi, H., H. Mackey, and G. McKay (2023). Adsorption of Methyl Orange from Water Using Chitosan Bead-Like Materials. *Molecules*, **28**(18); 6561

Amri, A., A. Lesbani, and R. Mohadi (2023). Malachite Green Dye Adsorption from Aqueous Solution Using a Ni/Al Layered Double Hydroxide-Graphene Oxide Composite Material. *Science and Technology Indonesia*, **8**(2); 280–287

Amri, A., S. Wibiyan, A. Wijaya, N. Ahmad, R. Mohadi, and A. Lesbani (2024). Efficient Adsorption of Methylene Blue Dye Using Ni/Al Layered Double Hydroxide-Graphene Oxide Composite. *Bulletin of Chemical Reaction Engineering & Catalysis*, **19**(2); 181–189

Borah, A. R., M. Gogoi, R. Goswami, P. K. Nath, and S. Hazarika (2025). Chiral Ni-Al LH Nanoparticle Embedded Electrospun Nanofibrous Membrane with High and Stable Permeance for Enantioseparation of Ketoprofen. *Separation and Purification Technology*, **361**; 131443

Boucif, F., F. Bessaha, F. Bendahma, G. Bessaha, N. Mahrez, M. Sillanpää, and A. Khelifa (2025). Facile Synthesis and Modification of Layered Double Hydroxides (LDH) for Adsorption of Orange I and Acid Red 114 Dyes from Aqueous Solution: Performance and Mechanism Study. *Inorganic Chemistry Communications*, **178**; 114673

Dehmani, Y., D. S. Franco, J. Georgin, R. Mghaiouini, B. B. Mohammed, R. Kacimi, T. Lamhasni, E. C. Lima, N. El Messaoudi, and A. Sadik (2025). Towards a Deeper Understanding of the Adsorption of Methyl Orange on a Commercial Activated Carbon: Study of Impact Factors, Isotherm and Mechanism. *Environmental Surfaces and Interfaces*, **3**; 103–111

Dong, Y., J. Liang, J. Song, C. Liu, Z. Ding, W. Wang, W. Zhang, et al. (2024). Preparation of Biochar/Iron Mineral Composites and Their Adsorption of Methyl Orange. *RSC Advances*, **14**(46); 33977–33986

Duan, J., S. Liu, X. Xu, Y. Zhang, Z. Dong, Z. Nie, R. Liu, X. Ren, and B. Wang (2025). Alginate Aerogel with High Adsorption Performance for Copper Ions. *Colloids and Surfaces A: Physicochemical and Engineering Aspects*, **719**; 137054

Duddi, R., S. Dhiman, A. K. Singh, N. Kamboj, S. Kumar, et al. (2025). Hydrothermally Synthesised Porous NiAl-LDH As an Efficient Pseudocapacitive Material in Asymmetric Supercapacitors. *Hybrid Advances*, **8**; 100372

El Foulani, A.-A., S. Tarhouchi, I. Hammoudan, R. Saddik, A. Y. A. Alzahrani, and S. Tighadouini (2025). A Novel Hydrazide-Modified Silica Gel As a Promising Material for Adsorption of Methyl Orange from Aqueous Solutions: Experiments and Theoretical Insights. *Results in Surfaces and Interfaces*, **18**; 100455

Etim, E. E., S. Yakubu, A. Terhembe, and L. J. Moses (2024). Investigations on the Biosorption of Nickel Using Tea Leaves and Tea Fibre (*Camellia sinensis*) As Adsorbents: Thermodynamics, Isotherms and Kinetics. *Discover Chemistry*, **1**(1); 3

Fu, S., Z. Xie, R. Wang, H. Zou, S. Lian, and R. Guo (2023). Combined Disposal of Methyl Orange and Corn Straw Via Stepwise Adsorption-Biomethanation-Composting. *Journal of Environmental Management*, **344**; 118358

Hammood, Z. A. and A. A. Mohammed (2024). Adsorption of Tetracycline from an Aqueous Solution on a CaMgAl-Layer Double Hydroxide/Red Mud Composite: Kinetic, Isotherm, and Thermodynamic Studies. *Environmental Nanotechnology, Monitoring & Management*, **22**; 101018

Han, J. H., D. H. Keum, V. Kothuri, Y.-J. Kim, H. C. Kwon, D. H. Kim, H. S. Jung, and S. G. Han (2024). Enhancing Emulsion, Texture, Rheological and Sensory Properties of Plant-Based Meat Analogs with Green Tea Extracts. *Food Chemistry: X*, **24**; 101807

Hariprasath, K., M. Priyadharshini, P. Balaji, R. Thangappan, T. Pazhanivel, et al. (2024). Electrode Engineering Strategies

for Boosting the Performance of NiCoAl-LDH in Supercapacitor Application. *Chemical Physics Letters*, **856**; 141584

Hashem, M. A., S. F. Rahman, S. R. Sium, M. Maoya, M. M. Miem, A. A. Mimi, and M. E. H. Zahin (2025). Thermally Activated Adsorbent Derived from Kitchen Biowaste for Treatment of Tannery Wastewater. *Cleaner Chemical Engineering*, **11**; 100156

Hezari, S., A. Olad, and A. Dilmaghani (2022). Modified Gelatin/Iron-Based Metal-Organic Framework Nanocomposite Hydrogel As Wound Dressing: Synthesis, Antibacterial Activity, and Camellia Sinensis Release. *International Journal of Biological Macromolecules*, **218**; 488–505

Hosseinpour, E. and A. Rahbar-Kelishami (2025). Cationic Surfactant Modified NaY Zeolite: Preparation, Investigating the Effect of Surfactant Concentration, and Application for Methyl Orange Adsorption from Aqueous Solution. *Journal of Environmental Chemical Engineering*, **13**(3); 116406

Jin, C., J. Yang, R. Zuo, W. Li, J. Wang, and J. Xu (2025). Adsorption Behavior and Mechanism of MnMgAl-Layered Double Hydroxide for the Removal of V(V): Experiments and DFT Calculation. *Process Safety and Environmental Protection*, **198**; 107187

Leng, Y., J. Li, J. Liu, F. Chang, Z. Li, Y. Huang, W. Xiong, B. Wu, B. Han, H. Chen, et al. (2025). Adsorption of Methyl Parathion on Four Various Microplastics in Aqueous Solution: Kinetics, Isotherms and Molecular Dynamics Simulations. *Gondwana Research*, **144**; 33–48

Lesbani, A., N. Ahmad, R. Mohadi, I. Royani, S. Wibiyan, Y. Hanifah, et al. (2024). Selective Adsorption of Cationic Dyes by Layered Double Hydroxide with Assist Algae (*Spirulina platensis*) to Enrich Functional Groups. *JCIS Open*, **15**; 100118

Li, Y.-J., T.-T. Qi, Y.-N. Dong, W.-H. Hou, G.-W. Chu, L.-L. Zhang, and B.-C. Sun (2022). Synthesized Ni/MMO Catalysts via Ultrathin Ni-Al-LDH in a Rotating Packed Bed for Hydrogenation of Maleic Anhydride. *Fuel*, **326**; 125035

Ma, Q., X. Han, J. Cui, Y. Zhang, and W. He (2022). Ni Embedded Carbon Nanofibers/Ni-Al LDHs with Multicomponent Synergy for Hybrid Supercapacitor Electrodes. *Colloids and Surfaces A: Physicochemical and Engineering Aspects*, **649**; 129270

Martins, N. J. and O. W. Perez-Lopez (2025). Tuning the Composition of Ni-Al-LDH Catalysts for Low-Temperature CO_2 Methanation. *Fuel*, **381**; 133594

Milovanovic, S., I. Lukic, N. Krgovic, V. Tadic, Z. Radovanovic, K. Tyśkiewicz, and M. Konkol (2024). Selection of Processing Parameters for the Integrated Supercritical CO_2 Extraction from Green Tea Leaves and Extract Impregnation onto Starch-chitosan Based Films. *The Journal of Supercritical Fluids*, **206**; 106163

Mishra, A., D. Singh, R. S. Singh, V. Mishra, M. Kumar, and B. S. Giri (2024). Performance Study of the Bioreactor for the Biodegradation of Methyl Orange Dye by Luffa Immobilized Stenotrophomonas Maltophilia and Kinetic Studies: A Sustainable Approach. *Groundwater for Sustainable Development*, **27**; 101378

Mubarak, M. F., T. A. Yousef, S. A. Salim, M. Khairy, E. A. Kamoun, and T. Mahmoud (2025). Meta-Kaolinite Metal Oxide Quaternary Composite for Layered Double Hydroxide Applied to a New Frontier in Adsorption Technology: Synthesis, Adsorption Performance and Kinetics Study. *Inorganic Chemistry Communications*, **178**; 114647

Pan, X., N. Zhao, H. Shi, H. Wang, F. Ruan, H. Wang, and Q. Feng (2025). Biomass Activated Carbon Derived from Golden Needle Mushroom Root for the Methylene Blue and Methyl Orange Adsorption from Wastewater. *Industrial Crops and Products*, **223**; 120051

Popat, P. R., A. Y. Alyami, G. K. Inwati, B. A. Makwana, M. A. Alreshidi, J. S. Algethami, M. Abbas, and K. K. Yadav (2024). Enriched Adsorption of Methyl Orange by Zinc Doped Lithium Manganese Oxides Nanosorbent. *Inorganic Chemistry Communications*, **161**; 112016

Purbasari, A., D. Ariyanti, and E. Fitriani (2023). Adsorption of Methyl Orange Dye by Modified Fly Ash-based Geopolymer–Characterization, Performance, Kinetics and Isotherm Studies. *Journal of Ecological Engineering*, **24**(3); 90–98

Qiu, Z., Y. Zhang, X. Lv, and J. Dang (2025). High-Capacity Biomass-based Composite Aerogel for Efficient Multi-Ion Adsorption of Vanadium, Molybdenum, and Nickel. *Separation and Purification Technology*, **368**; 132990

Ramutshatsha-Makhwedzha, D., A. Mavhungu, M. L. Moropeng, and R. Mbaya (2022). Activated Carbon Derived from Waste Orange and Lemon Peels for the Adsorption of Methyl Orange and Methylene Blue Dyes from Wastewater. *Heliyon*, **8**(8); e09930

Roy, N., S. A. Alex, N. Chandrasekaran, K. Kannabiran, and A. Mukherjee (2022). Studies on the Removal of Acid Violet 7 Dye from Aqueous Solutions by Green ZnO@Fe_3O_4 Chitosan–Alginate Nanocomposite Synthesized Using *Camellia sinensis* Extract. *Journal of Environmental Management*, **303**; 114128

Sajai, N., B. Soubai, S. El Khaider, A.-i. Chham, R. Fakhreddine, I. Mechnou, and S. Krimi (2025). Valorization of Calcium Phosphate Glasses: A Sustainable and Eco-Friendly Approach to Methylene Blue Dye Adsorption from Wastewater. *Results in Surfaces and Interfaces*, **19**; 100525

Tcheka, C., M. M. Conradie, V. A. Assinale, and J. Conradie (2024). Mesoporous Biochar Derived from Egyptian Doum Palm (*Hyphaene thebaica*) Shells As Low-cost and Biodegradable Adsorbent for the Removal of Methyl Orange Dye: Characterization, Kinetic and Adsorption Mechanism. *Chemical Physics Impact*, **8**; 100446

Waheed, T., P. Min, S. Shujaat, S. Haq, S. ud Din, M. K. Hossain, F. U. Rehman, A. Syed, A. H. Bahkali, L. S. Wong, et al. (2024). Enhanced Photocatalytic Performance of Cr/Ni/Mg/Al Layered Double Hydroxides Against Methyl Orange in Aqueous Solution. *Desalination and Water Treatment*, **319**; 100495

Wibiyan, S., I. Royani, N. Ahmad, and A. Lesbani (2024). Assessing the Efficiency, Selectivity, and Reusability of ZnAl-layered Double Hydroxide and Eucheuma Cottonii Composite in Removing Anionic Dyes from Wastewater. *Inorganic Chemistry Communications*, **170**; 113347

Wijaya, A., N. Ahmad, L. Hanum, E. Melwita, and A. Lesbani (2025). *Spirogyra sp.* Macro-Algae-Supported NiCr-LDH Ad-

sorbent for Enhanced Remazol Red Dye Removal. *Results in Surfaces and Interfaces*, **18**; 100427

Xie, C.-r., Y.-x. Song, G. Yang, C.-g. Sun, X. Luo, and T. Wu (2024). Porous Carbon Derived from MOF-235 for the Adsorption of Methyl Orange with High Capacity. *Materials Today Communications*, **41**; 110843

Yang, P., J. Bi, H. Zhang, and Z. Wu (2024). EDTA-Interlayer Modified Mg/Fe Layered Double Hydroxides for Enhanced Adsorption of Methyl Orange: Adsorption Performance and Mechanism Study. *Process Safety and Environmental Protection*, **186**; 1387–1396

Zhang, Q., Z. Wu, and S. He (2025). Preparation of Superhydrophilic and Underwater Superoleophobic Composite Graphene Aerogels and Their Performance in Dye Adsorption and Oil/Water Separation. *Carbon*, **241**; 120384

Zhou, A., L. Zhu, Y. Chen, J. Wang, and Y. Liu (2025). Fast Adsorption of Low-concentration Ammonia Nitrogen by Persulfate-Modified Carbon Materials: Structure Influence, Performance, and Mechanism. *Environmental Research*, **278**; 121680